IMPACT EXPERIMENTS FOR CRATER SIZE SCALING LAWS ON RUBBLE-PILE ASTEROIDS.

Y. Yamamoto[1], M. Arakawa[1], M. Yasui[1], S. Hasegawa[2], Y. Yokota[1], [1]Kobe University, Kobe, Japan, (184s425s@stu.kobe-u.ac.jp), [2] Institute of Space and Astronautical Science, JAXA, Japan

Introduction: Recent planetary explorations showed that rubble-pile asteroids were covered with boulders with size distributions and low strength. Moreover, it was found that the number of craters on asteroid Itokawa was small. The craters less than 10 m in the diameter were absent [1]. The mechanism for the lack of small craters is thought to be an armoring effect [2]. The reduction of the crater formation efficiency due to the armoring effect is caused when the impacts occur under the following condition: The target grain size is comparable or larger than an impactor size and the target grains are partially disrupted during the impact [3,4,5]. However, on the surface of asteroid Ryugu, which are covered with boulders having various sizes and low strength [6,7], the craters were formed in the same size as predicted in the conventional crater scaling law for gravity-controlled regime [8,9]. Therefore, a detailed study to elucidate the effects of the size distribution and the strength of boulders on the armoring effect would be necessary for the study of impact craters formed on rubble-pile asteroids. In this study, we conducted impact experiments on granular targets composed of low strength and coarse-grains to study the effects of size distribution and strength on the crater size scaling law.

Experimental methods: Cratering experiments were conducted by using vertical gas gun sets at Kobe University and ISAS. Granular targets were prepared by using weathered tuff granules with the size of 1 to 4 mm (small particle) and the size of 1 to 4 cm (large particle). The crush strength of these tuff particles was measured to be about 60 kPa and 13 kPa, respectively. A spherical projectile with the size of 3 mm (stainless steel, zirconia, alumina, glass, and nylon) was launched at the impact velocity from 40 to 200 m/s, and a spherical projectile with the size of 2 mm (tungsten carbide, copper, stainless steel, zirconia, titan, aluminum, polycarbonate, and nylon) was launched at the impact velocity from 1.2 to 4.5 km/s. These projectiles were impacted on the target surface at the normal direction. Impact cratering phenomena were observed by a high-speed camera at the frame rate of 10^3-10^5 fps. After each shot, the crater morphology was observed by using the 2D laser displacement, and the diameter and the depth were measured. Impact-induced seismic waves were measured by using three accelerometers (a specific frequency is 30 kHz) at different positions from the impact point, and a data logger was used to record the seismic data through charge amplifiers (the data acquisition rate was 100 kHz).

Results: *Crater size scaling law*. Fig. 1 shows the relationship between the crater radius and the kinetic energy of projectiles for different targets and projectiles.

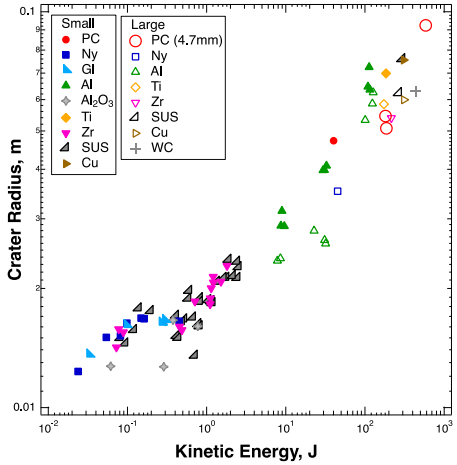

Fig1: Crater radius vs kinetic energy of the projectile. The closed and open symbols show the results of small particle targets and those of large particle targets, respectively.

As a result, the crater radius increases with increasing kinetic energy of a projectile (E_k), except for the region of the E_k between 0.1 and 0.6 J, the crater radius was almost constants in this region. This trend did not depend on the projectile materials but the crater radius of the large particle target was smaller than that of the small particle target at the same E_k.

The π-scaling law [8] was applied to our experimental results to study the effects of the target particle size and the strength on the cratering efficiency. Fig. 2 shows the relationship between the normalized radius and the normalized gravity.

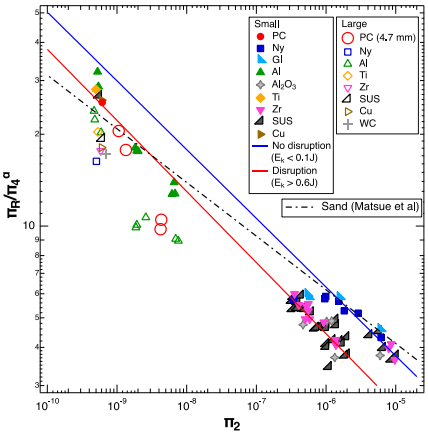

Fig2: Normalized crater radius π_R vs normalized gravity π_2 for various projectiles and two types of targets. The two solid lines show the fitting lines shown by Eqs. (1) and (2). The dashed line shows the previous results of quartz sand [10].

We first noticed that the cratering efficiency for the large particle targets is lower than that for the small particle target. Secondary, we found that the data of the small particle targets was separated into two regions with a clear offset, depending on the impact velocity and the projectile material. This offset might be caused by the dissipation of the projectile kinetic energy due to the disruption of tuff particles. The disruption should be caused by the impact pressure calculated from the impact velocity and the projectile density. These data of small particle targets can be fitted by the different empirical equations as follows:

$\pi_R \pi_4^{-\alpha} = 10^{-0.55\pm0.12}\, \pi_2^{-0.23\pm0.02}$ (blue line) (1),

$\pi_R \pi_4^{-\alpha} = 10^{-0.75\pm0.21}\, \pi_2^{-0.25\pm0.06}$ (red line) (2).

These results in Fig. 2 showed that the cratering efficiency of weak coarse grain targets was affected by not only the particle size but also the disruption of tuff particles by the impact pressure. Therefore, π-scaling law for crater size should be improved to include the mechanism for the reduction in the crater formation efficiency due to the disruption of the target grains and the size ratio of the projectile to the target grain.

Discussions: In order to construct an improved scaling relationship for the crater size including the effects of the grain disruption, we followed the idea proposed by Mizunati et al. (1983) [11], which introduced a late-stage effective energy, *I*, and *I* was defined as the product of impact pressure and projectile volume. We then consider the total energy required for the disruption of target grains estimated from the number of disrupted grains and the potential energy of the crater cavity, and it is assumed as follows,

$k_1 \rho g D^4 + k_2 \varepsilon \alpha \delta_t d^3 = aI$ (3),

Where *D* is crater size, g is the gravitational acceleration, ε is an energy per unit mass of grains, ρ is bulk target density, α is number of the disrupted target grains, δ_t is bulk density of one target grain, and *d* is average radius of one target grain. Replacing Eq. (3) with the typical crater size, D^*, we obtain the following relationship,

$$I = k_3 \left\{ \rho \left(\frac{D}{D^*}\right)^4 + \alpha \delta_t \left(\frac{d}{D^*}\right)^3 \right\} \quad (4),$$

where k_3 is constant. At $D > D^*$, the crater formation process is dominated by the gravity, and at $D < D^*$ it is dominated by the strength. The k_3 and D^* were determined from our experimental results for $I < 0.05$ J because no disruption of target grains was observed: We then obtained to be $k_3 = 1.6\times10^{11}$ and $D^* = 200$ m. Using Eq. (4) and our results, we also determine the relationship between α and *I* using a power-law equation of $\alpha = A \cdot I^n$, where *A* and *n* are the constants. We obtained to be $A = 20$ and $n = 0.98$ for the small grain targets, and $A = 0.5$ and $n = 0.98$ for the large grain targets. Eq. (4) is rewritten as follows,

$$D = D^* \left[\frac{1}{\rho} \left\{ \frac{1}{k_3} - AI^n \delta_t \left(\frac{d}{D^*}\right)^3 \right\} \right]^{1/4} \quad (5).$$

By using this relationship, we can introduce the effect of target grain disruption, *f*, into the π-scaling law for crater size,

$$\pi_R^* = f \cdot k_4\, \pi_2^{-a} \pi_4^b,$$

$$f = \left\{ 1 - k_3 A I^{n-1} \delta_t \left(\frac{d}{D_2^*}\right)^3 \right\}^{1/4} \quad (4).$$

Fig. 3 shows the relationship between π_R and π_2

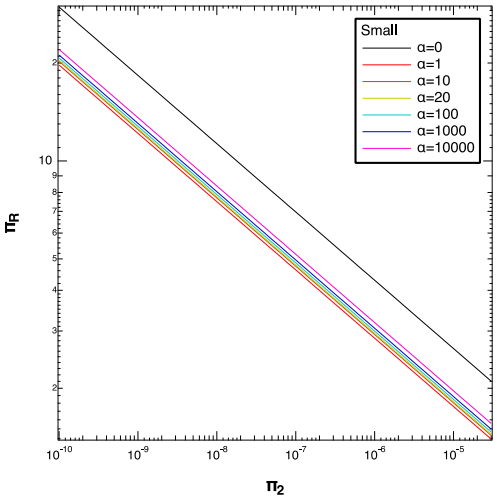

Fig. 3: Simulating that a φ=3 mm steel is used as a projectile.

calculated by Eq. (6) for 3-mm-sized SUS projectile. As shown in Fig. 3, the π_R of $\alpha \geq 1$ was smaller than that of $\alpha = 0$ due to the disruption of the target grain. In addition, since the π_R of $\alpha \geq 1$ are almost the same, it is noticed that the degree of reduction in cratering efficiency due to the armoring effects do not depend on the number of disrupted target grains so much.

References: [1]Hirata et al. (2009), Icarus, 200, 486-502. [2]Chapman and Merline (2002), Icarus, 155, 104-118. [3] Güttler et al. (2012) *Icarus, 220,1040-1049.* [4] Tatsumi & Sugita (2002) *Icarus, 300, 227-248.* [5]Yasui et al. (2022) JGR Planets, 127, Issue 8. [6] Michikami et al. (2019), *Icarus, 331, 179-191.* [7] Grött et al. (2019), *Nature Astron, 3, 971-976.* [8] Holsapple & Housen (2011) *Icarus, 211,* 856–875. [9]Arakawa et al. 2020, Science, 368(6486), 67–71. [10] Matsue et al. (2020), *Icarus, 338, 113520.* [11]Mizutani et al. (1983), JGR, 88, A835-A945